

Theranostics

1

2

Supplementary Materials for

3

4

**Apolipoprotein E, low-density lipoprotein receptor, and
immune cells control blood-brain barrier penetration by
AAV-PHP.eB in mice**

6

7

8

Bao-Shu Xie^{1,4#}, Xin Wang^{2#}, Yao-Hua Pan^{1#}, Gan Jiang³, Jun-Feng Feng¹,

9

and Yong Lin^{1*}

10

11 # These authors contributed equally to this work.

12 * **To whom correspondence should be addressed:**

13 Yong Lin, MD, PhD, Department of Neurological Surgery, Ren Ji Hospital, School of

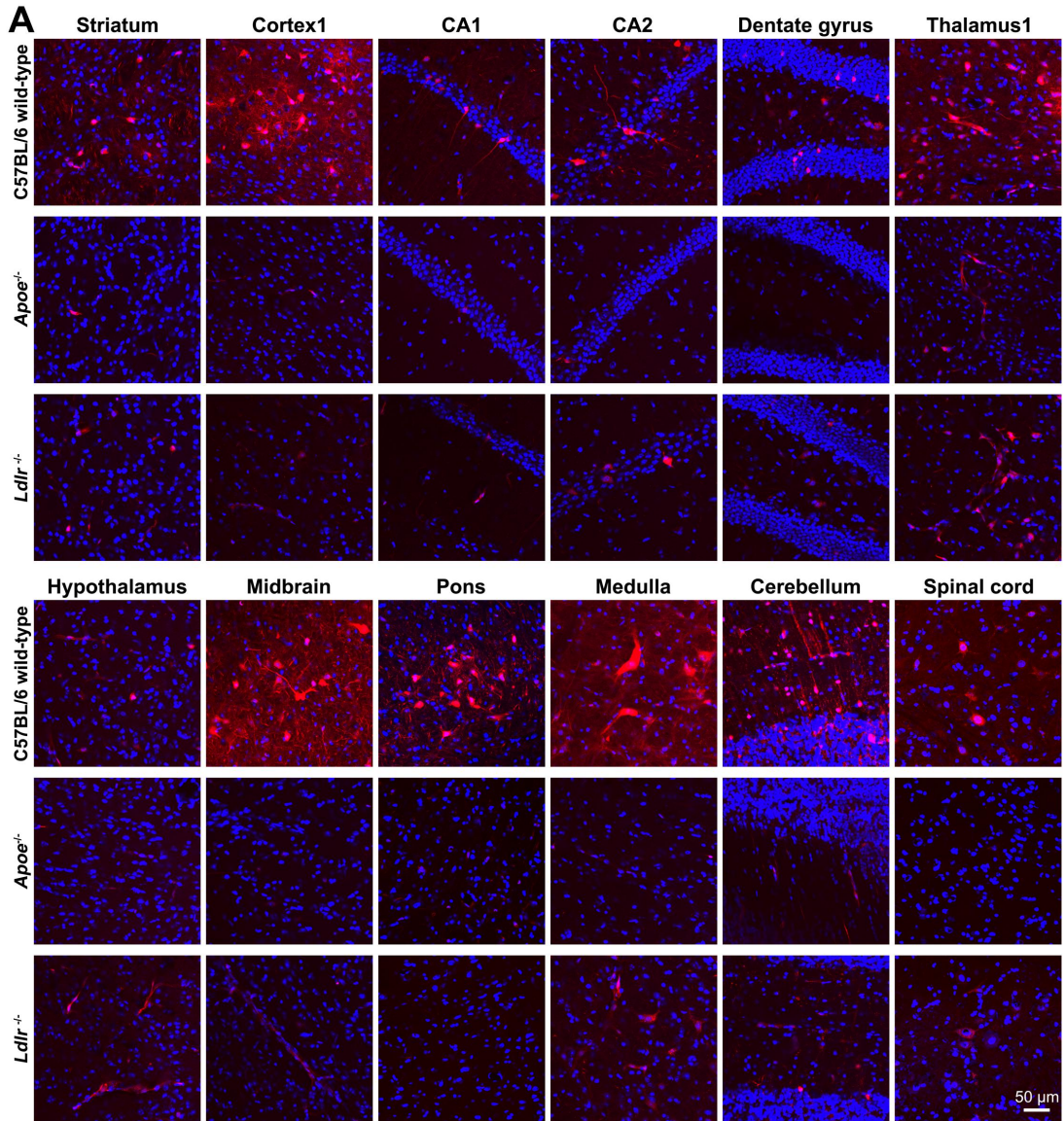
14 Medicine, Shanghai Jiao Tong University, 160 Pujian Road, Shanghai 200127, P.R.

15 China. Tel: +86 (21) 6838 3982. Email: yonglin1996@hotmail.com

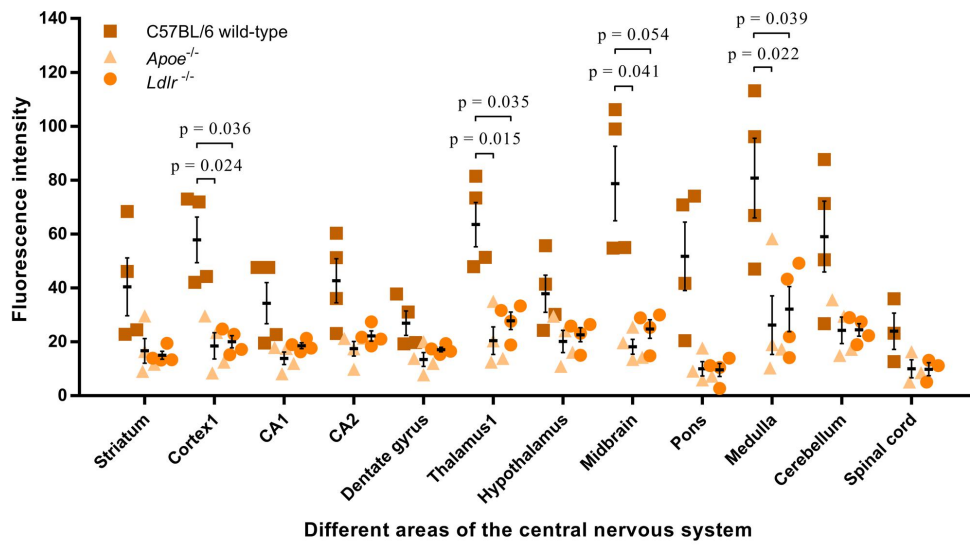
16

17 **This PDF file includes:** Figures S1 to S6

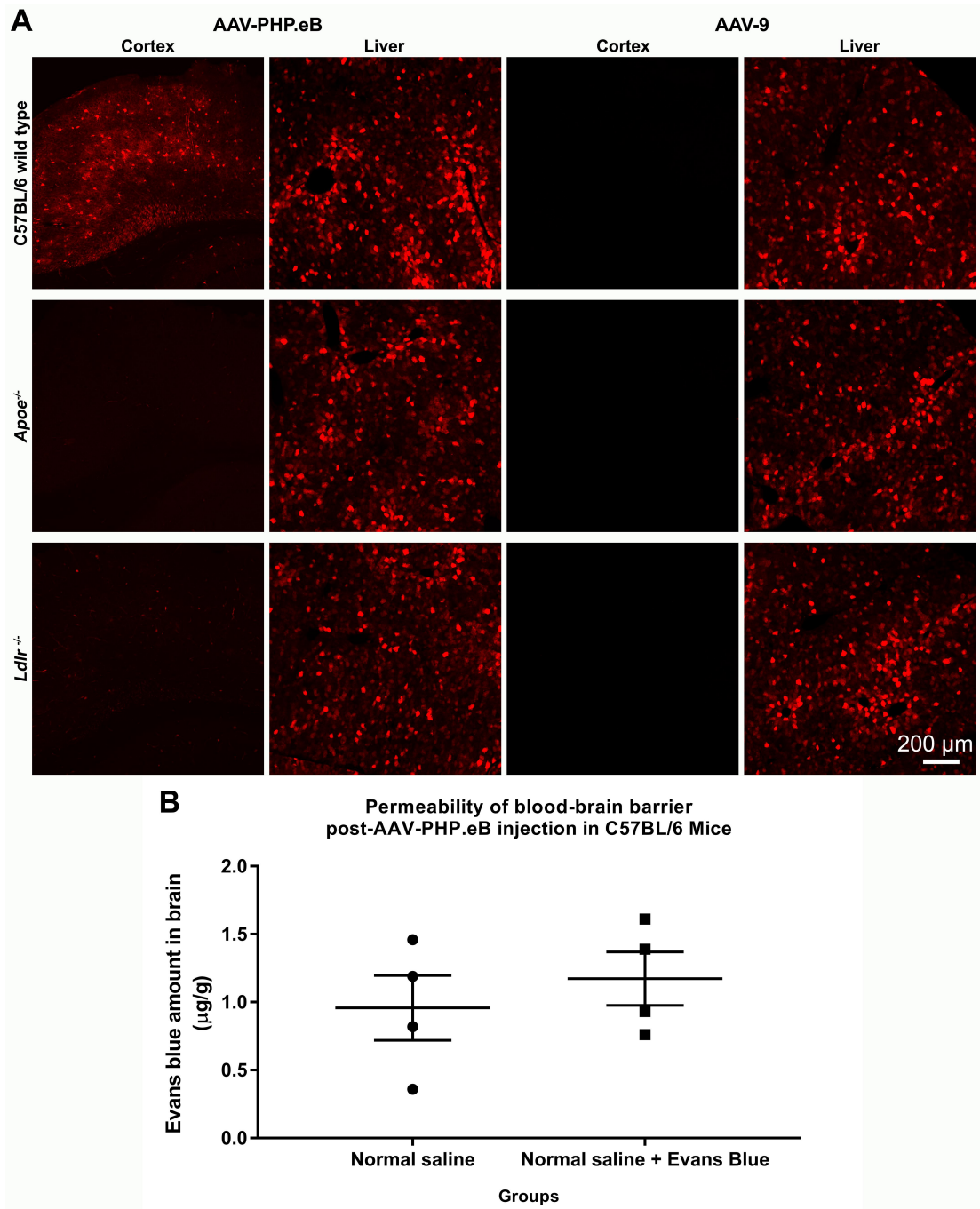
18



B Roles of ApoE and LDLR in C57BL/6 mouse in AAV-PHP.eB transduction



1 **Figure S1 | Transduction of intravenous AAV-PHP.eB into various brain regions**
2 **of C57BL/6 wild-type, *ApoE*^{-/-} and *Ldlr*^{-/-} mice. (A)** Representative fluorescent
3 images of the indicated tissues in the indicated mice following intravenous
4 administration of AAV-PHP.eB. The blue fluorescence indicates Hoechst nuclear
5 staining. **(B)** Quantification of the red fluorescence intensity in the indicated mice and
6 brain regions 3 weeks after the AAV-PHP.eB administration (n = 4 for each group).
7 For the comparison of C57BL/6 wild-type with either *ApoE*^{-/-} or *Ldlr*^{-/-} mice, p values
8 were determined by Tukey post-hoc test (medulla) or Games-Howell post-hoc test (all
9 other regions). Data are mean ± s.e.m.



1

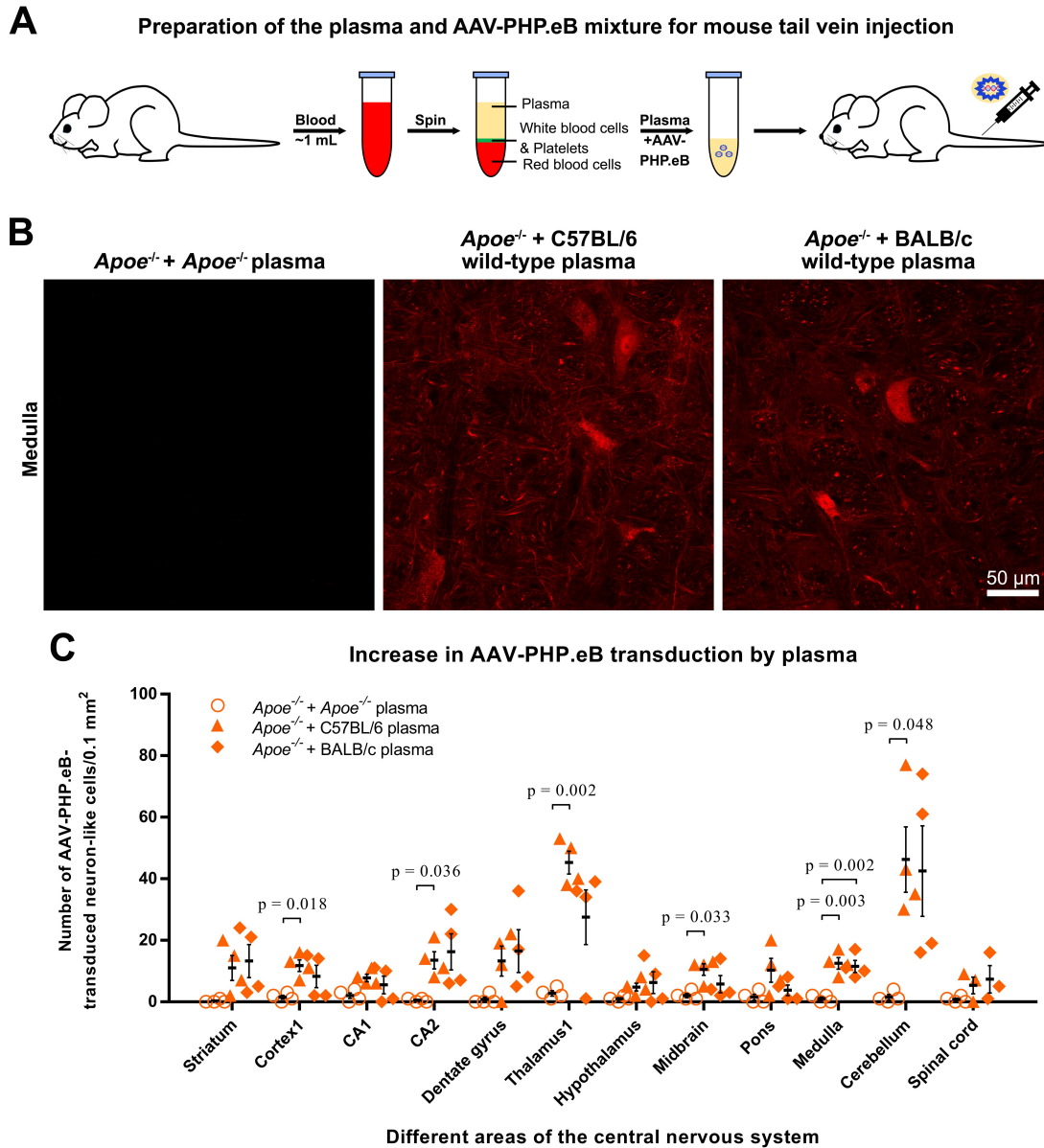
2 **Figure S2 | Brain and liver transduction of AAV-PHP.eB and AAV-9 and effect of**
 3 **AAV-PHP.eB on the permeability of the blood-brain barrier in mice. (A)**

4 Representative images of the AAV-PHP.eB and AAV-9 transduction in the indicated

5 tissues in the indicated mice. While transducing to both the brain and the liver (red

6 fluorescence) in wild-type C57BL/6 mice, AAV-PHP.eB is able to transduce only the

1 liver cells in *ApoE*^{-/-} or *Ldlr*^{-/-} mice (n = 3 for each group). In contrast, AAV-9
2 transduces the liver cells, but fails to transduce brain cells in all three mouse
3 genotypes (n = 3 for each group). **(B)** Evaluation on the permeability of the
4 blood-brain barrier after the AAV-PHP.eB injection. Intravenously injected
5 AAV-PHP.eB does not significantly increase the barrier permeability, measured by
6 Evans Blue infiltration, in C57BL/6 mice (n = 4 for each group).



1

2 **Figure S3 | Effect of plasma on the central nervous system transduction of**

3 **intravenous AAV-PHP.eB in *ApoE*^{-/-} mice. (A) Schematic showing plasma isolation**

4 **from wild-type mouse blood and preparation of AAV-PHP.eB expressing the *mScarlet***

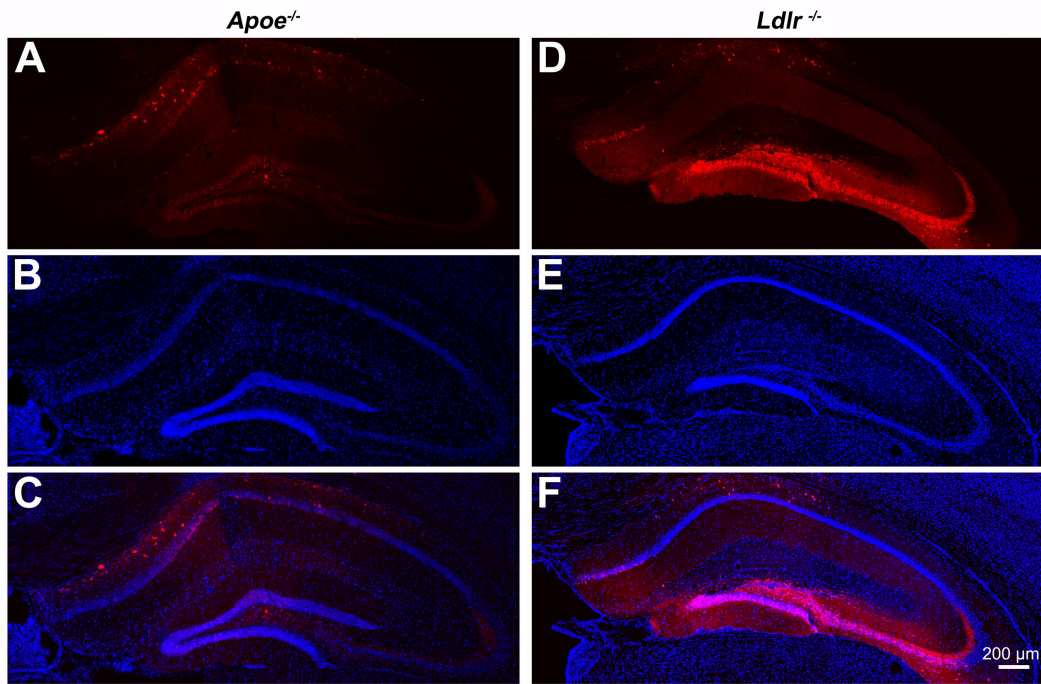
5 **gene mixed with plasma. Thirty minutes after being mixed with ApoE-containing**

6 **plasma prepared from either C57BL/6 or BALB/c mice, AAV-PHP.eB was**

7 **administered intravenously to *ApoE*^{-/-} mice. (B) Representative images showing**

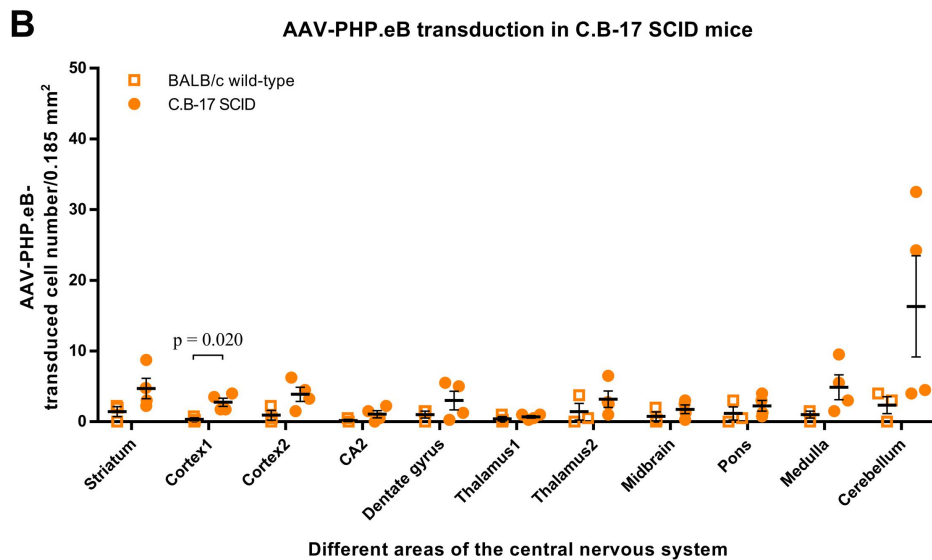
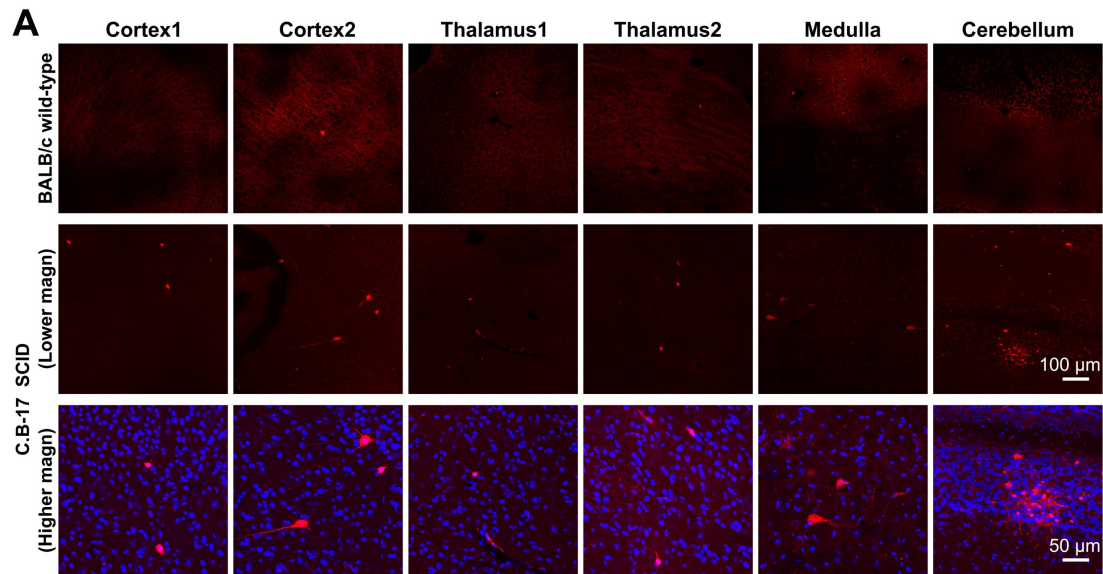
8 **transduction in the medulla regions 3 weeks after systemic delivery of AAV-PHP.eB**

1 plus plasma. Images from an *ApoE*^{-/-} mouse which was not treated with plasma are
2 shown as a negative control. **(C)** Quantification of the fluorescence intensity of the
3 indicated brain regions. The p values were determined by one-way ANOVA. The
4 means \pm s.e.m are indicated (n = 4 for each group).



1

2 **Figure S4 | Comparison of the local transduction of AAV-PHP.eB in the brains in**
3 ***Apoe*^{-/-} and *Ldlr*^{-/-} mice.** Representative fluorescent images (red, **A** and **D**) of the
4 hippocampi (**B** and **E**) in *Apoe*^{-/-} (**A-C**) and *Ldlr*^{-/-} (**D-F**) mice following the
5 stereotactic microinjection of AAV-PHP.eB into the dentate gyrus. **A** and **B** are
6 merged in **C**, and **D** and **E** in **F**. The blue fluorescence indicates Hoechst nuclear
7 staining. n = 2 for each group.



1

2 **Figure S5 | Transduction of intravenous AAV-PHP.eB to the brain of in C.B-17**

3 **SCID mice lacking both T and B cells. (A)** Representative images of the indicated

4 tissues, 3 weeks after the intravenous AAV-PHP.eB administration to BALB/c

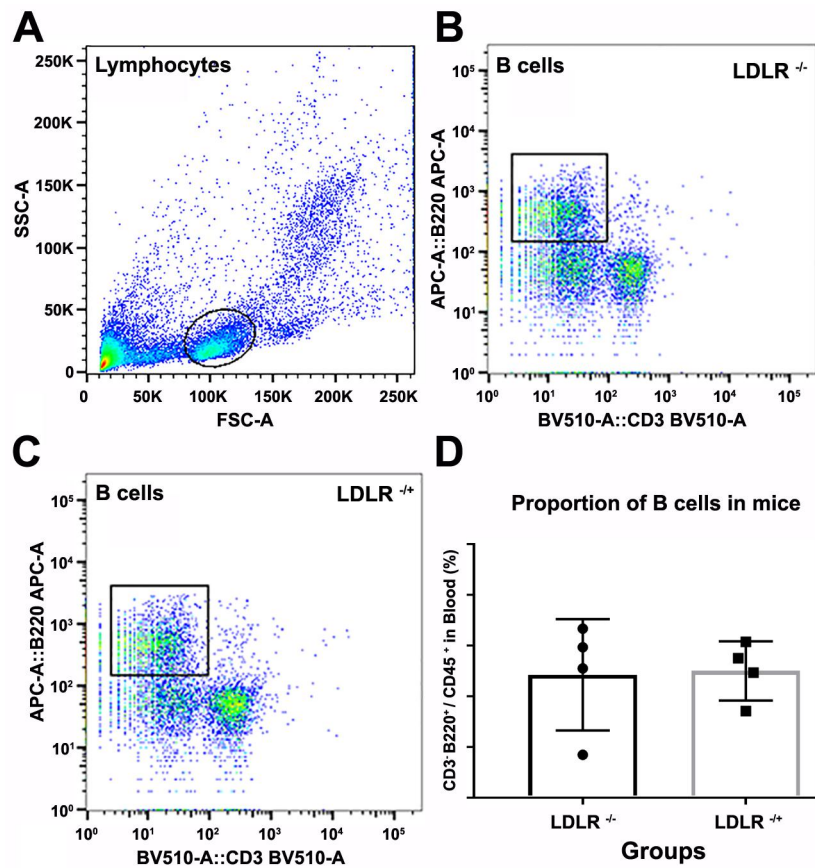
5 wild-type and C.B-17 SCID mice. The blue fluorescence indicates Hoechst nuclear

6 staining. magn: magnification. **(B)** Analyses of the AAV-PHP.eB transduction in the

7 indicated areas of BALB/c (n = 3) and C.B-17 SCID mice (n = 4), 3 weeks after the

8 AAV-PHP.eB injection; the p value was determined by two-tailed Student's t-test.

9 Data are mean ± s.e.m.



1

2 **Figure S6 | Lymphocyte and B cell populations in the spleens of *ldlr*^{-/-} and *ldlr*^{+/+}**
 3 **mice. (A-C)** Flow cytometry analyses of lymphocytes in the spleen (A) and of B cells
 4 in *ldlr*^{-/-} (B) and *ldlr*^{+/+} (C) mice. (D) Quantification of the ratios of CD3⁺B220⁺ B
 5 cells to CD45⁺ lymphocytes. The means ± s.e.m are indicated (n = 4 for each group).
 6 The p values > 0.05 (two-tailed Student's t-test).